Electronic Supplementary Material (ESI) for Journal of Materials Chemistry A.

Supplementary Information

Dehydration kinetics of the synthesis of high-nickel cathode materials used in lithium ion batteries

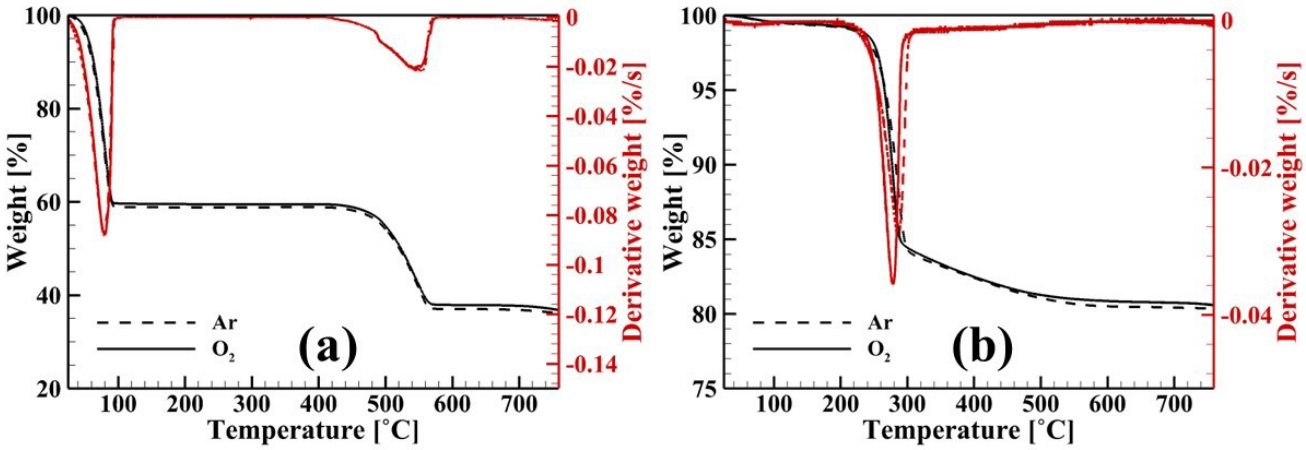

Fig. S1. The comparison of TGA measurement in the different atmospheres of Ar and O_2 for (a) $LiOH \cdot H_2O$ and (b) $Ni_xCo_yMn_z(OH)_2$ precursor.

Table S1. The elemental composition of $Ni_xCo_yMn_z(OH)_2$ measured by ICP-OES.

Element [%]	Ni	Co	Mn
ICP-OES	88.169	5.115	6.716

Table S2. The materials and space groups that are expressed in the subscripts of crystal planes.

Subscripts	Materials	Space group
L, C	Lithium hydroxide monohydrate	C 1 2/m 1
L, P	Lithium hydroxide	P 4/n m m
L, F	Lithium oxide	F m -3 m
N, P	Transition metal hydroxide	P -3 m 1
N, R	Transition metal oxide	R -3 m

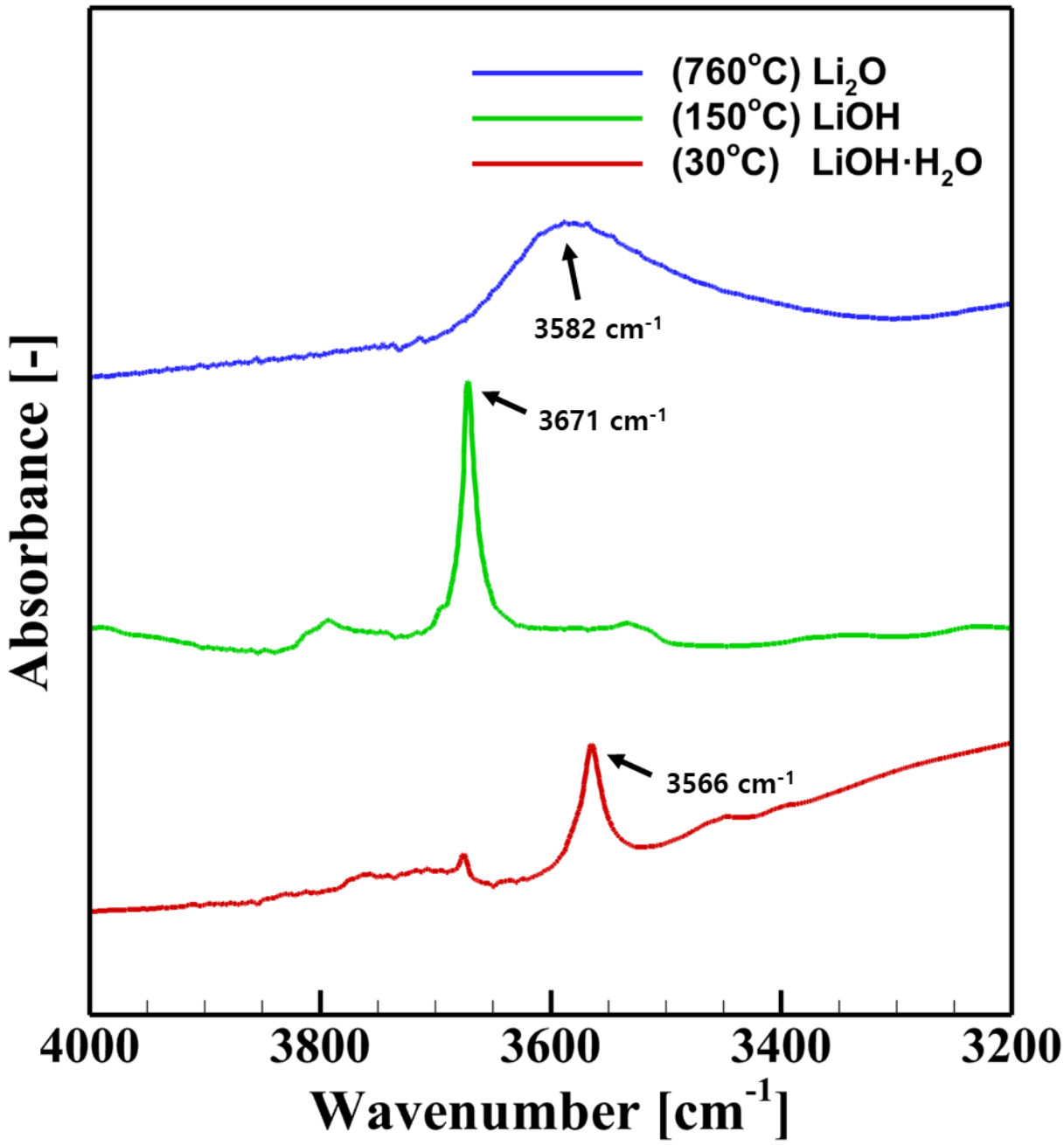

Fig. S2. IR spectrum measured by in-situ DRIFT at the temperature of 30°C, 150°C and 760°C.

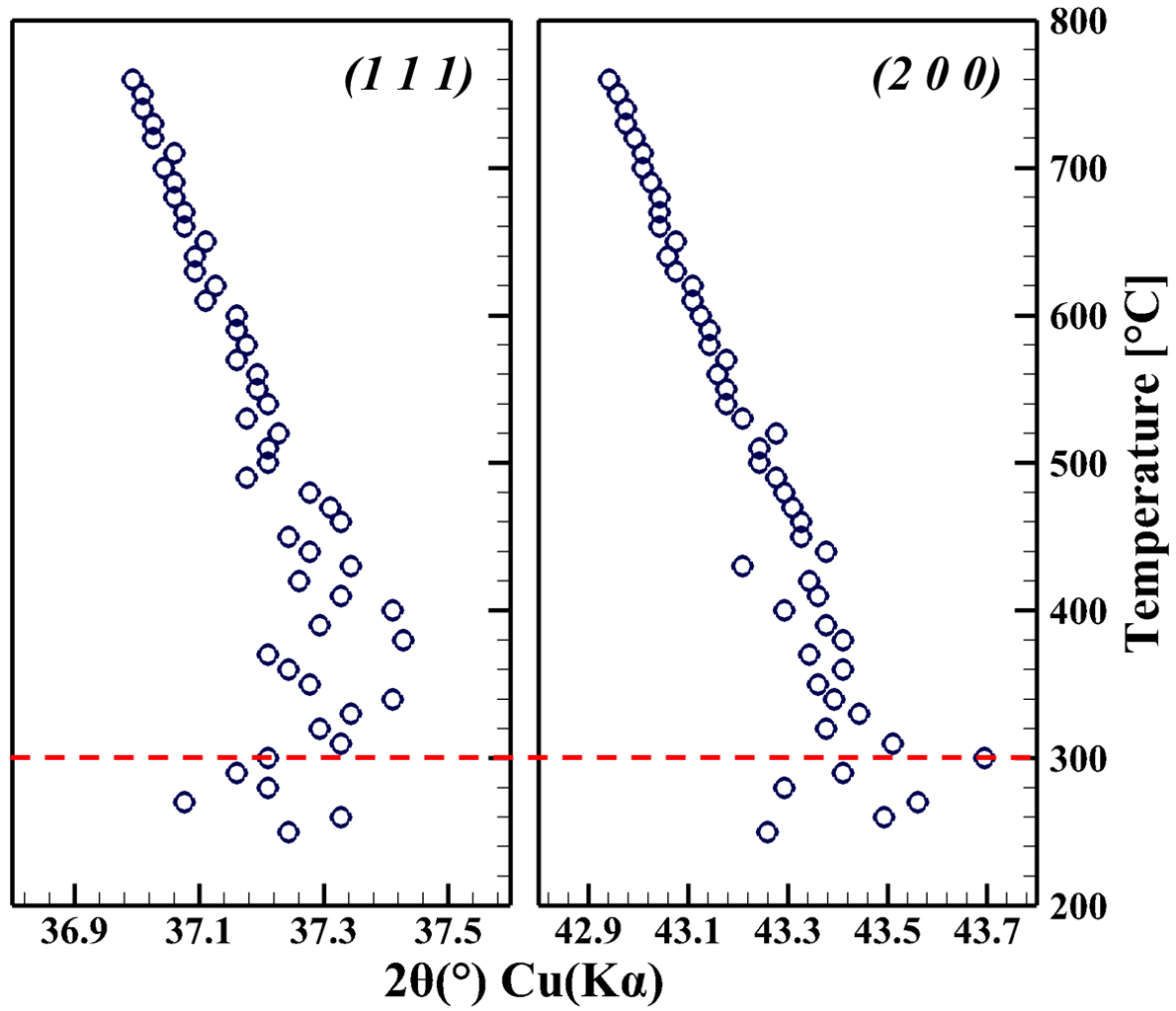

Fig. S3. A schematic diagram for the main peak (111) and (200) shifts in the in-situ XRD measurements of the $Ni_xCo_yMn_z(OH)_2$ precursor.

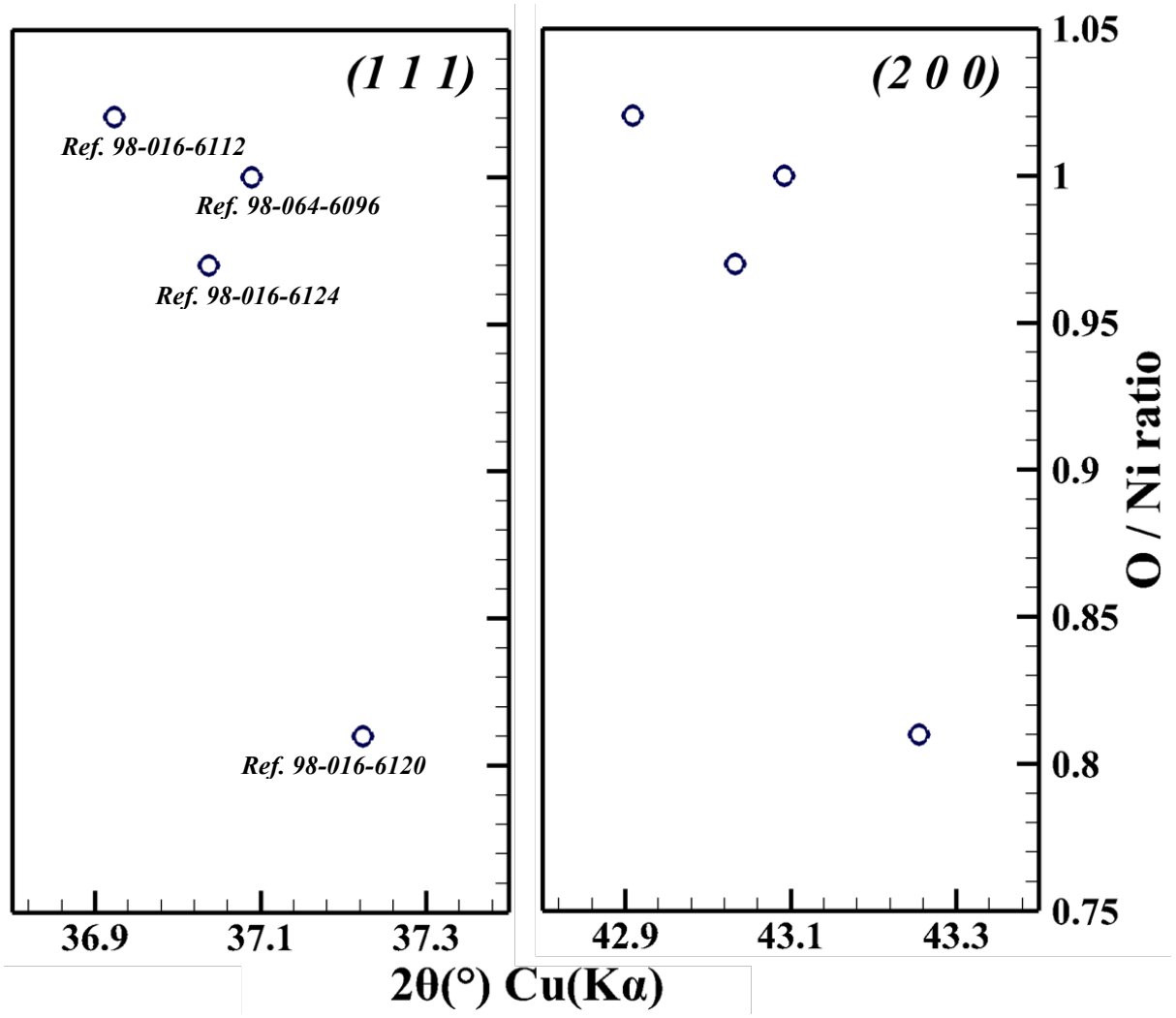

Fig. S4. A schematic diagram for the main peak (111) and (200) shifts with respect to O/Ni ratio of NiO_x based on reference.

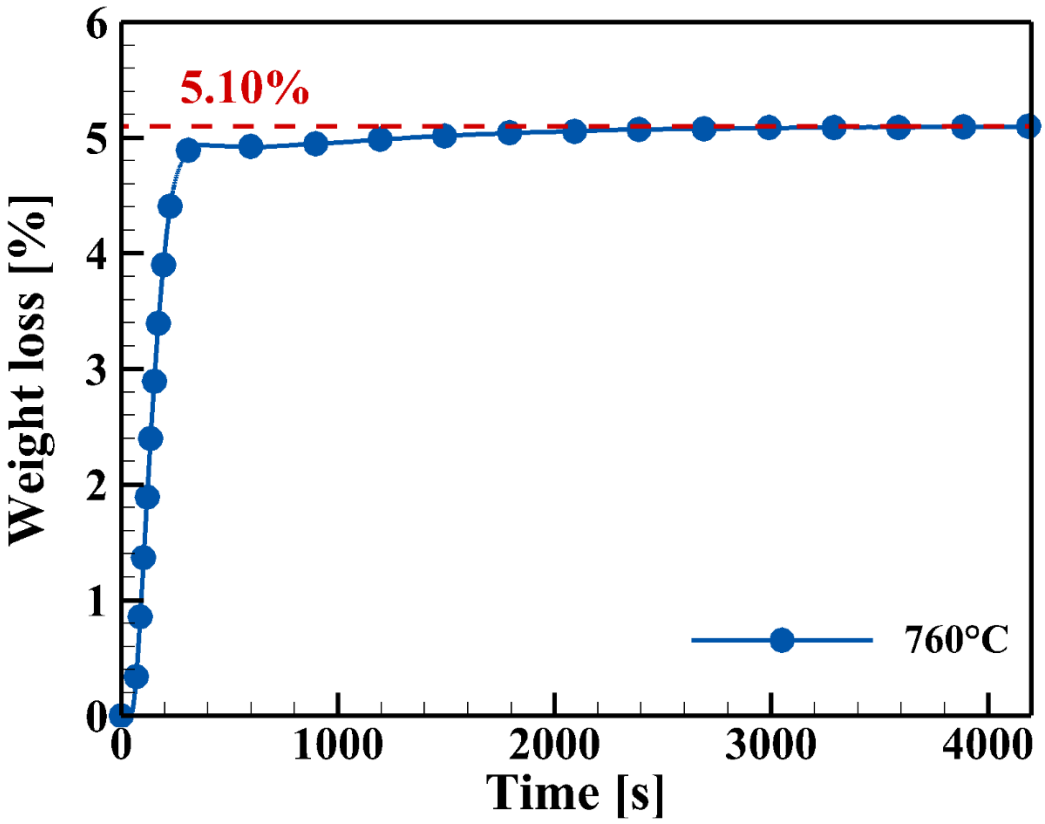

Fig. S5. TGA results at the isothermal temperature of 760°C for $R_{2\text{-}2}$: decomposition of $Ni_xCo_yMn_zO_{1.25}$.

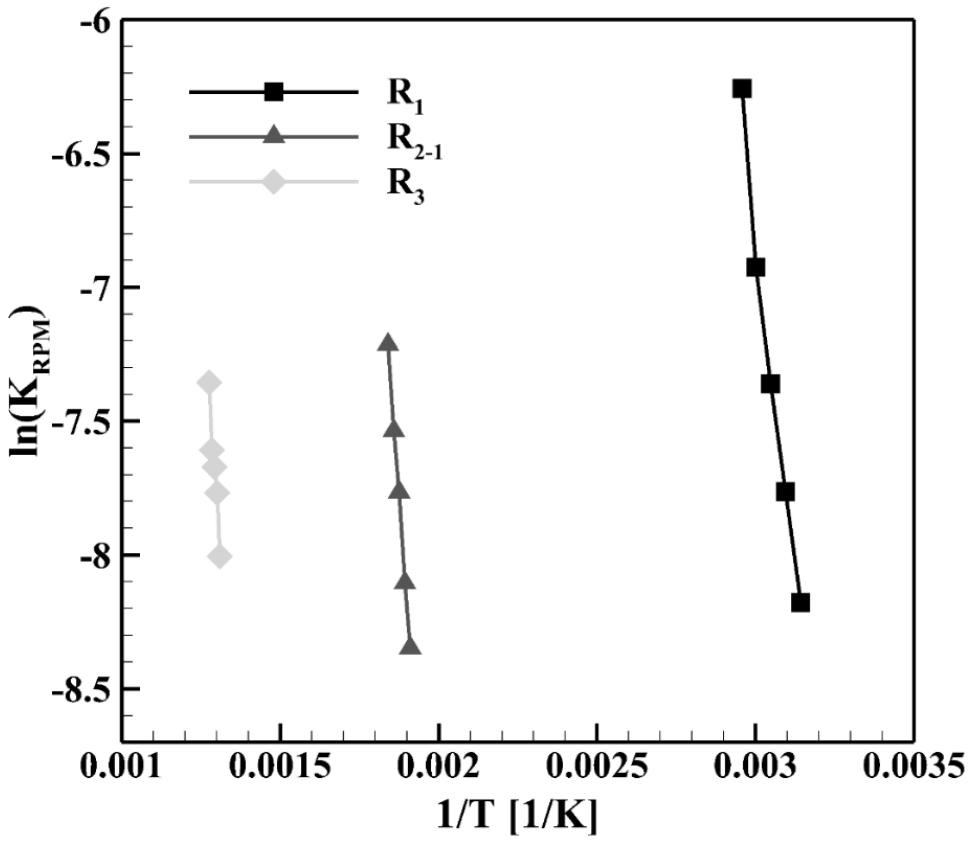

Fig. S6. Arrhenius curves for the dehydration reactions of the precursors.